Statistical Estimation of High-Resolution Surface Air Temperature from MODIS over the Yangtze River Delta, China

Yi SHI[1], Zhihong JIANG[2*], Liangpeng DONG[1,3], and Suhung SHEN[4]

1 *Key Laboratory of Meteorological Disaster, Ministry of Education/Collaborative Innovation Center on Forecast and Evaluation of Meteorological Disasters, Nanjing University of Information Science &Technology, Nanjing* 210044, *China*
2 *Joint International Research Laboratory of Climate and Environment Change/Collaborative Innovation Center on Forecast and Evaluation of Meteorological Disasters, Nanjing University of Information Science &Technology, Nanjing* 210044, *China*
3 *Wuhan Central Meteorological Observatory, Wuhan* 430074, *China*
4 *George Mason University, Fairfax, Virginia* 22030, *USA*

(Received May 27, 2016; in final form February 16, 2017)

ABSTRACT

High-resolution surface air temperature data are critical to regional climate modeling in terms of energy balance, urban climate change, and so on. This study demonstrates the feasibility of using Moderate Resolution Imaging Spectroradiometer (MODIS) land surface temperature (LST) to estimate air temperature at a high resolution over the Yangtze River Delta region, China. It is found that daytime LST is highly correlated with maximum air temperature, and the linear regression coefficients vary with the type of land surface. The air temperature at a resolution of 1 km is estimated from the MODIS LST with linear regression models. The estimated air temperature shows a clear spatial structure of urban heat islands. Spatial patterns of LST and air temperature differences are detected, indicating maximum differences over urban and forest regions during summer. Validations are performed with independent data samples, demonstrating that the mean absolute error of the estimated air temperature is approximately 2.5°C, and the uncertainty is about 3.1°C, if using all valid LST data. The error is reduced by 0.4°C (15%) if using best-quality LST with errors of less than 1 K. The estimated high-resolution air temperature data have great potential to be used in validating high-resolution climate models and other regional applications.

Key words: remote sensing, surface air temperature, land surface temperature, land cover type, Moderate Resolution Imaging Spectroradiometer (MODIS)

Citation: Shi, Y., Z. H. Jiang, L. P. Dong, et al., 2017: Statistical estimation of high-resolution surface air temperature from MODIS over the Yangtze River Delta, China. *J. Meteor. Res.*, **31**(2), 448–454, doi: 10.1007/s13351-017-6073-y.

1. Introduction

The surface air temperature (T_a) is a key element for studying energy cycles, hydrological cycles, and climate variations, as well as agricultural productivity, climate, health, and so on. Traditionally, T_a is measured 1.5–2 m above ground at meteorological stations. However, in remote areas, stations are relatively sparse. High resolution T_a is a key forcing for driving hydrological and ecological models, such as crop growth models (Foley et al., 2005) and epizootic disease research models (Connor et al., 1998). There is also a demand for high-resolution T_a when validating regional weather research and forecasting models over regions with complex land use (Pan and Li, 2011; Kusaka et al., 2012). Traditional methods involve spatially interpolating station T_a to grid points of a desired resolution; for instance, the inverse distance weighting, nearest neighbor, regression, triangular irregular network, B-spline, and Kriging methods are popularly used in the geosciences (Li and Heap, 2008). However, most of these interpolation methods are linear and the accuracy of results may be poor if stations are sparsely located.

Space borne sensors on satellites receive reflected ra-

Supported by the National Natural Science Foundation of China (41230528), National (Key) Basic Research and Development (973) Program of China (2010CB428505), and Priority Academic Program Development of Jiangsu Higher Education Institutions (PAPD).

*Corresponding author: zhjiang@nuist.edu.cn.

diance from surface objects in different channels. Algorithms have been developed to retrieve the land surface temperature (LST) or skin temperature based on remotely sensed radiance data. These remotely sensed data have a much better spatial coverage than those from ground stations. Although it is difficult to retrieve T_a directly via available visible and infrared channels (Czajkowski et al., 2000), efforts have been made to derive T_a from satellite measurements. For example, the contextual temperature–vegetation index (TVX) method uses the negative relationship between the vegetation index and LST for estimating T_a based on the hypothesis that the temperature of a dense vegetation canopy is close to air temperature (Prihodko and Goward, 1997). The TVX method provides an estimate for T_a with a root-mean-square error in the range of 3–4°C; however, it is sensitive to the vegetation density, with the error increasing over sparsely vegetated regions.

Another method is to estimate T_a through analysis of the correlation between station T_a and satellite LST. Using data from Meteosat over South Africa, Cresswell et al. (1999) found that the daily minimum T_a has a good relationship with nighttime LST, indicating that nighttime LST is about 3.3–4.2°C lower than minimum T_a. Mostovoy et al. (2006) calculated the statistical relationship between Moderate Resolution Imaging Spectroradiometer (MODIS) daytime/nighttime LST and daily maximum/minimum T_a over Mississippi, USA, reporting rather high correlation coefficients. Colombi et al. (2007) investigated the feasibility of using MODIS LST to estimate T_a over the Italian Alps and documented satisfactory results. Note, however, that the regression coefficients in the above studies are quite different.

Shen and Leptoukh (2011) calculated the correlation between MODIS LST and station T_a over a relatively large region in central–eastern Eurasia and northern China. There are also many other studies on remotely sensed data in China. Qi et al. (2006) estimated T_a using Terra satellite data, analyzed the relationship between Normalized Difference Vegetation Index (NDVI) and LST, and indicated that the relationship between LST and NDVI is not good at night and the negative linear correlation between NDVI and LST can be observed in daytime over the plains. Using data from 2340 stations in China and the corresponding LST data from NOAA's Advanced Very High Resolution Radiometer, Han et al. (2012) established a statistical model involving a number of impact factors to calculate the maximum T_a from LST, and produced satisfactory results. Zhang et al. (2011) compared T_a estimates derived from daytime and nighttime LST observed by MODIS with daily maximum, minimum, and mean T_a observations collected at 678 standard Chinese meteorological stations in 2003. They found that the models using nighttime LST were better than those using daytime LST. Xu et al. (2015) used observed T_a data at 33 automatic meteorological stations at 10-min intervals and MODIS T_a products in 2011, and established a linear relationship between the observed T_a and the satellite remotely sensed LST. They found the multiple regression equation to be best. It is recognized that the correlation between daytime LST and maximum T_a depends significantly on the type of land surface, whereas the correlation between nighttime LST and minimum T_a is relatively consistent over all land surface types.

The Yangtze River Delta region in eastern China has undergone rapid economic development during the last three decades. This has resulted in a high fraction of urban cover and heterogeneous T_a, which cannot be resolved by using station observations. In order to use regional climate models to study the climate variation, agricultural response, air quality, and health issues associated with developing megacities, it is important to obtain T_a observations at a sufficiently high resolution for regional modeling and corresponding validation. Considering the complexity of the land surface in the Yangtze River Delta region, this study adopts the algorithm of Shen and Leptoukh (2011) to derive T_a. The procedure for estimating high resolution T_a is presented below.

2. Study region and data

The Yangtze River Delta refers to a triangular-shaped territory, including Shanghai, southern Jiangsu Province, and northern Zhejiang Province in China (Fig. 1). After the Chinese economic reform program, which began in 1978, the rapid urban development in the area has given rise to what may be the largest metropolitan area in the world. In this study, the area covers 29°–33°N, 118°–122°E, including more than 10 cities, such as Shanghai, Nanjing, Suzhou, Wuxi, Changzhou, Hangzhou, and Ningbo. The Yangtze River Delta has a subtropical marine monsoon climate, with hot and humid summers, cool and dry winters, and warm spring and autumn seasons.

The station T_a data are from the National Meteorological Information Center, China Meteorological Administration, which are carefully quality-controlled (Xu et al., 2013). Stations over inland water surfaces (lakes, rivers), or with incomplete temporal coverage due to migration, are not used. Ultimately, a total of 87 stations from 2001 to 2010 are used in this study.

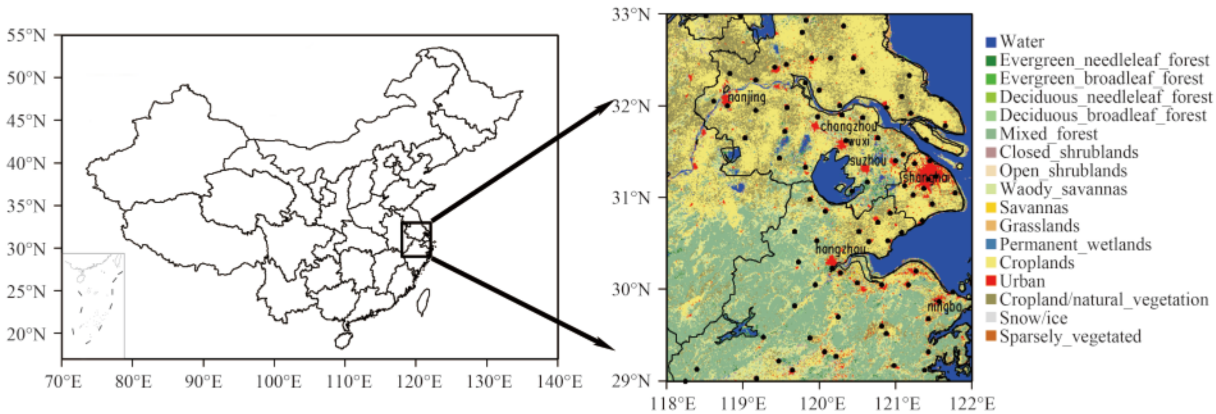

Fig. 1. Location of the study region and a zoomed map depicting the meteorological station locations (black dots) and MODIS land cover types over the Yangtze River Delta, China.

For the same period, daily MODIS Terra LST data at a resolution of 1 km (MOD11A1.005) and the 16-day MODIS vegetation index product (MYD13A2-NDVI) are obtained from NASA's Land Processes Distributed Active Archive Center (LP DAAC) (Wan, 1999, 2006; Wan et al., 2004; Wan and Li, 2008; Shen and Leptoukh, 2011).

Additionally, the yearly MODIS Land Cover Types (LCT) product is used in this study to determine the surface type at each meteorological station. LCT is a combined Terra and Aqua product at a resolution of 500 m (MCD12Q1.005) (Strahler et al., 1999; Shen and Leptoukh, 2011).

The original data files for MOD11A1.005, MYD13A2-NDVI, and MCD12Q1.005 are stored as 10° × 10° tiles in a sinusoidal projection due to the large size of the dataset. For ease of use, all data are preprocessed by stitching the original tiled data files into a single file over the study region, and are projected onto a cylindrical equidistant projection by using the nearest-point method in the MODIS Reprojection Tool, version 4.0, provided by LP DAAC. Figure 1 shows the MODIS LCT of 2001 and the location of the meteorological stations over the study area, indicating cropland or cropland/natural vegetation over most northern areas, and mixed forest over most southern mountain areas.

3. Regression models

Due to the complexity of the land surface in the study region, the station locations are classified by using the nine-point method, as follows. First, find the nearest point in the LCT data to the station location and define it as the center point. If the center point is urban (LCT = 13), and over 65% (6 out of 9 points) are of urban type, the station is classified as an urban station. If less than 20% (less than 2 out of 9 points) are urban, the station is classified as a rural station, that is, a rural type is defined according to the land surface type of the majority of the 9 stations. The remaining stations are classified as suburban. Considering that the number of stations is limited, some similar types are combined, resulting in eight new land cover types (NLCTs), as listed in Table 1.

Among the 87 stations, urban and suburban types are

Table 1. Restructured land surface types in the Yangtze River Delta region and the number of stations belonging to each type in 2008 and 2009

NLCT	Number of stations in 2008	Number of stations in 2009	New type	Original index and type
1	2	2	Evergreen forest	1 Evergreen needle leaf forest 2 Evergreen broadleaf forest
2	2	3	Deciduous forest	3 Deciduous needle leaf forest 4 Deciduous broadleaf forest 5 Mixed forest
3	3	5	Shrub land	6 Closed shrub land 7 Open shrub land
4	8	6	Savanna	8 Woody savanna 9 Sananna
5	14	16	Cropland	12 Cropland
6	37	37	Urban	13 Urban
7	8	5	Cropland/natural vegetation	10 Grassland 14 Cropland/natural vegetation
8	13	13	Suburban	–

dominant, accounting for 43% and 15%, respectively. Stations over cropland and cropland/natural vegetation together amount to 26%, while stations of forest type are very limited. The results show that more than 50% of the stations are located in urban- and suburban-type areas. Although the total number of stations in the Yangtze River Delta is relatively large compared to other regions of China, stations in rural areas, particularly mountain areas, are very sparsely distributed. Thus, the statistical interpolation of T_a in this region may be urban-biased.

The daytime LST (LST hereafter) values at all quality levels, co-located to stations, are extracted for 2008 and 2009, and converted to units of °C. The linear regression coefficients are calculated between the station maximum T_a (T_a hereafter) and LST over each LCT, as shown in Table 2. The results show that the correlation coefficients are high for all LCTs, varying from 0.92 over deciduous forest to 0.95 over cropland, at the 95% confidence level. In most rural areas, such as forest, cropland, and cropland/natural vegetation, T_a is equal to or higher than LST. Over urban areas, T_a is higher than LST at the lower-value end (winter), but opposite at the higher-value end (summer). This is likely due to the lower specific heat capacity and higher heat conductivity of urban surfaces. It is clear that the linear regression coefficients vary with LCT significantly. Figure 2 shows scatter plots between T_a and LST for selected types: deciduous forest (NLCT = 2), cropland (NLCT = 5), and urban (NLCT = 6). The linear regression ($T'_a = a \times \text{LST} + b$) is employed to estimate T_a, where T'_a is the estimated T_a, and a and b are the coefficients of each NLCT, as listed in Table 2. The correlation between nighttime LST and minimum T_a is also found to be high, and it does not depend on the surface type.

Independent data samples from the years 2001 to 2003 are used for validation. For each station, based on classified types, T'_a is calculated with the linear equation by using the corresponding coefficients. Then, T'_a and T_a are compared in terms of the mean absolute error (MAE) and standard deviation (STD), as shown in Table 2. The results show that the MAE varies from 2.2°C over cropland/natural vegetation to 2.9°C over evergreen forest. The uncertainty of the estimated data (i.e., STD) varies from 2.9°C over cropland/natural vegetation to 3.4°C over deciduous forest. In summary, the average MAE of T'_a is 2.5°C, with an uncertainty of 3.1°C.

To examine the influence of the quality of the input LST on the accuracy of T'_a, the LST data are filtered by taking only the values flagged as being best quality, i.e., the data with errors less than 1 K. The linear regression coefficients and error of T'_a are recalculated. Table 2 shows the MAE and STD of daily T'_a from LST at all quality levels and best quality levels, separately. As we can see, the errors are reduced if using best-quality LST

Table 2. Regression relationships between the maximum surface air temperature and daytime land surface temperature, mean absolute error (MAE), and standard deviation (STD) at all quality levels and the best quality levels. The letters a and b denote the linear regression coefficients at all quality levels

NLCT	All quality levels				Best quality levels	
	a	b	MAE (°C)	STD (°C)	MAE (°C)	STD (°C)
1	0.92	2.65	2.86	3.05	2.67	2.47
2	0.97	3.73	2.8	3.43	2.2	2.75
3	0.95	0.18	3.48	3.1	2.74	2.43
4	0.94	2.28	2.46	3.07	2.08	2.57
5	0.98	0.53	2.28	2.96	2.1	2.66
6	0.89	1.91	2.41	3.11	2.06	2.71
7	0.93	1.36	2.24	2.88	2.03	2.54
8	0.95	1.07	2.56	3.31	2.77	3.43

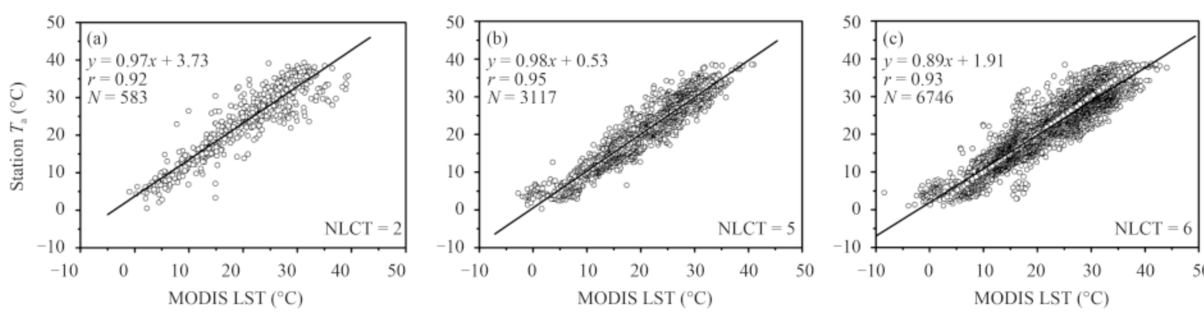

Fig. 2. Scatter plots between maximum T_a and MODIS daytime LST over (a) deciduous forest (NLCT = 2), (b) cropland (NLCT = 5), and (c) urban (NLCT = 6). The solid line is the linear regression $T'_a = a \times \text{LST} + b$.

data. The average improvement in MAE is around 0.4°C (15%), with a maximum improvement of around 0.7°C (20%) over shrub land.

The TVX method is also used to estimate the maximum air temperature (T_{max}) in summer. In Fig. 3, based on all the pixels for the summers of 2001, 2002, 2003, 2008, and 2009, the correlation coefficient between MODIS NDVI and MODIS LST is –0.276, so there is no significant linear correlation between NDVI and LST. Therefore, we select pixels with the highest values of NDVI, defined as those showing values equal to or greater than the 90th percentile, in each dataset. Based on the selected pixels, the correlation coefficient between NDVI and LST is –0.808 (Fig. 4), and a linear relationship between T_{max} and NDVI can be expressed by

$$T'_{max} = -9.3097\mathrm{NDVI} + 313.01, \tag{1}$$

where T'_{max} is the estimated T_{max}.

We calculate T'_{max} of the 87 stations based on the NDVI and Eq. (1), and compare the results with the observed values of T_{max}. The MAE between T'_{max} and T_{max} is 4.92°C and the STD is 6.004°C, which is larger than that from the regression method (Table 2, where the MAE is less than 3.48°C and the STD less than 3.43°C). Therefore, we surmise that the relationship between LST and T_{max} is better than that between NDVI and T_{max}, and the regression method between LST and T_{max} is better than the TVX method, over the Yangtze River Delta.

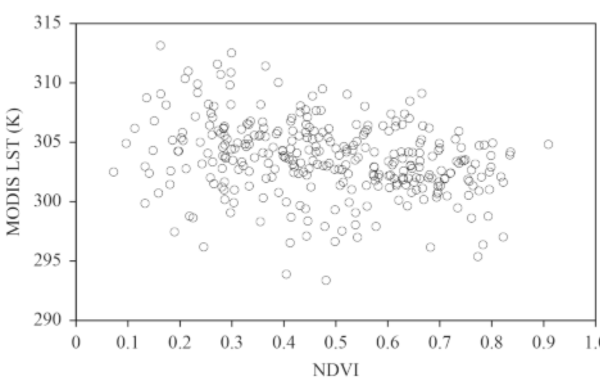

Fig. 3. Scatter plot between MODIS NDVI and MODIS LST for the summers of 2001, 2002, 2003, 2008, and 2009.

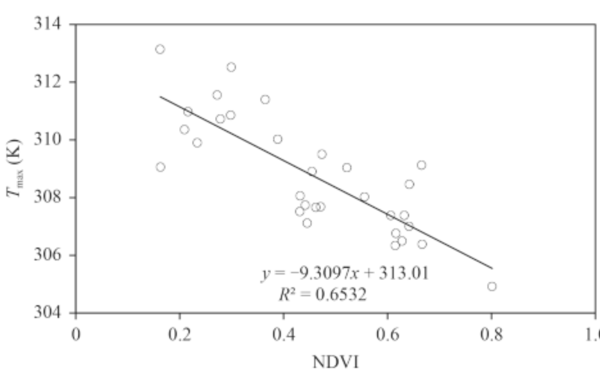

Fig. 4. Scatter plot between MODIS NDVI and T_{max}. The solid line is the linear regression.

4. High-resolution air temperature data

The daily T'_a from LST at a resolution of 1 km is calculated as follows: (1) the NLCT data at a resolution of 500 m are aggregated to 1 km; (2) the surface type of a grid point is defined according to the majority surface type; and (3) T'_a at each grid point is calculated by using the linear regression equation with coefficients of the corresponding NLCT.

To achieve a better spatial coverage, the LST at the best-quality levels is used to derive the daily T'_a. Although the error is reduced by 15%, the data points or spatial coverage are reduced significantly if using LST at the best-quality levels only.

Figure 5a shows the averages of daily T'_a in summers (June–August) for the 10-yr study period (2001–10). As we can see, daily T'_a is higher than 29°C in the Yangtze River Delta region, except for the southwestern and northwestern parts, and the temperature is closely related to the type of surface cover. The temperature is higher than 32°C over urban areas, such as Shanghai, Hangzhou, and Nanjing. However, daily T'_a is significantly lower over rural areas than over urban areas, by about 2°C, reflecting the urban heat island effect, and this is true for all 18 cities. The areal size of the elevated T'_a is proportional to the size of the city. For example, the areal size of the elevated T'_a over Shanghai is the largest among all cities, whereas the areal size of the elevated T'_a is much smaller over small cities, such as Changzhou. Also of note is that the temperature between cities (Shanghai, Suzhou, Wuxi, and Changzhou) is higher than in remote rural areas, resulting in a vast combined heat island. The lowest T'_a values appear over the southwestern (Tianmu Mountain) region, where the NLCT of most stations is evergreen forest or deciduous forest, and the temperature is lower than 29°C.

Figure 5b shows the average differences between LST and T'_a. As we can see, the differences are spatially nonuniform, with the largest differences over urban and forest LCTs. Over urban areas, LST is higher than T'_a. For example, LST is about 1°C higher than T'_a in Shanghai and adjacent areas, with the maximum difference being around 1.9°C. Over forest areas, LST is, however, lower than T'_a, such as over Tianmu Mountain in the southwest and Tiantai Mountain in the southeast, with a

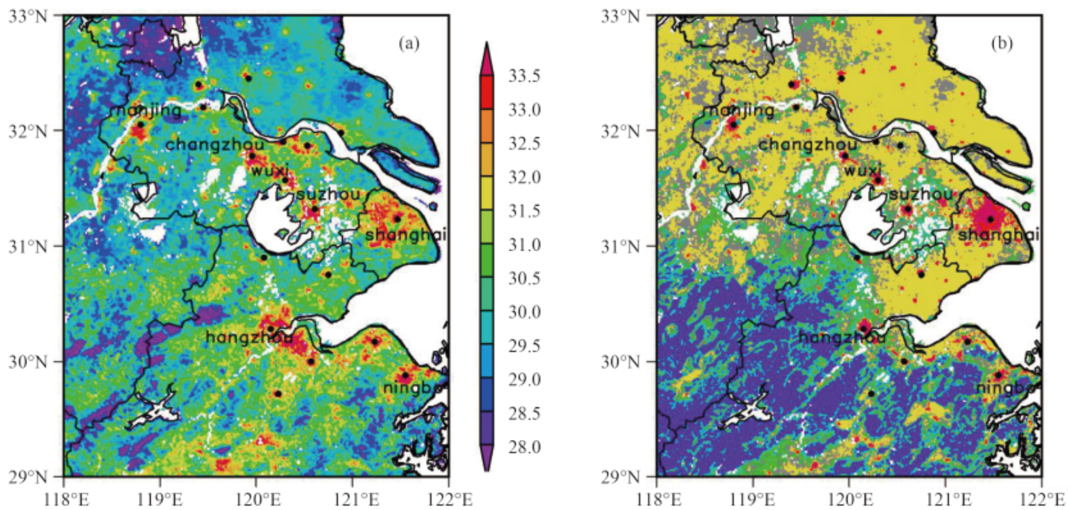

Fig. 5. (a) Daily estimated maximum surface air temperature for boreal summer (June–August) averaged from 2001 to 2010 over the Yangtze River Delta. (b) Difference between daytime land surface temperature and estimated maximum surface air temperature. Black dots denote the locations of cities.

maximum difference of around –2.7°C. This may be associated with the different heat capacity and heat conductivity of urban and forest areas. In summer, the concrete surface of urban areas is dry under a clear sky, heating faster than the air via the incoming irradiation; whereas, vegetation in forest areas is moist and heats slower than the air.

5. Conclusions and discussion

This study estimates the summertime daily maximum T_a at a resolution of 1 km over the Yangtze River Delta, China, based on remotely sensed daytime LST from MODIS-Terra via linear regression models. The models can also be used for calculating T_a in other seasons. It is found that the linear regression coefficients depend significantly on the land surface type. The correlation coefficients are high between MODIS daytime LST and station maximum T_a over all land cover types, varying between 0.92 and 0.95. Statistical errors of the estimated T_a are around 2.5°C in terms of MAE, and the uncertainty is around 3.1°C (STD), with the largest values over forest-type land cover in mountain areas, which may be associated with the lower number of data samples. If using best-quality LST (i.e., LST with an error of less than 1 K), the error of the estimated T_a can be reduced by around 15%. However, the problem with this is that the number of missing data points increases significantly when using best-quality data only. The TVX method is also used to estimate T_{max} in summer. In the TVX method, the MAE of T'_{max} is 4.92°C and the STD is 6.004°C. The regression method between LST and T_{max} is better than the TVX method over the Yangtze River Delta.

The mean summer estimated T_a at a resolution of 1 km shows in detail a clear spatial structure involving higher values in urban areas, moderate values in suburban areas, and lower values in remote rural areas. The results indicate that, in summer, LST exceeds T_a over urban areas, with a maximum difference of 1.9°C; however, the opposite is true over forest areas, with a maximum difference of –2.7°C. It is known that the spatial structure of urban heat islands cannot be observed by using statistical interpolation of data from stations, due to coarse resolution of observations. With the method presented in the present study, the derived high spatial resolution observational air temperature can be used in regional numerical models for studies of urban climate and air quality, as well as agricultural applications.

One potential problem is that T_a derived from MODIS LST may have missing data points due to instrument and algorithm limitations associated with gaps between swathes, cloudiness, heavy aerosols, and so on. These data gaps may be large during cloudy conditions, especially during the monsoon rainfall season. In addition, since LST data are available only under clear-sky conditions, the area and monthly or seasonal mean of the estimated T_a will likely be an overestimation or underestimation compared to under all-sky conditions. More studies on understanding the clear-sky biases and data gap filling are needed to obtain high resolution T_a data with complete spatial coverage.

Acknowledgments. The authors are grateful to the Monsoon Asia Integrated Regional Study (MAIRS) project and Giovanni system at NASA GES DISC (Goddard Earth Sciences Data and Information Servies Center) for their data exploration of MODIS high resolution land surface temperatures and other land products.

REFERENCES

Colombi, A., C. De Michele, M. Pepe, et al., 2007: Estimation of daily mean air temperature from MODIS LST in Alpine areas. *EARSeL*, **6**, 38–46.

Connor, S. J., M. C. Thomson, S. P. Flasse, et al., 1998: Environmental information systems in malaria risk mapping and epidemic forecasting. *Disasters*, **22**, 39–56, doi: 10.1111/1467-7717.00074.

Cresswell, M. P., A. P. Morse, M. C. Thomson, et al., 1999: Estimating surface air temperatures, from Meteosat land surface temperatures, using an empirical solar zenith angle model. *Int. J. Remote*, **20**, 1125–1132, doi: 10.1080/014311699212885.

Czajkowski, K. P., S. N. Goward, S. J. Stadler, et al., 2000: Thermal remote sensing of near surface environmental variables: Application over the Oklahoma mesonet. *The Professional*, **52**, 345–357, doi: 10.1111/0033-0124.00230.

Foley, J. A., R. DeFries, G. P. Asner, et al., 2005: Global consequences of land use. *Science*, **309**, 570–574, doi: 10.1126/science.1111772.

Han, X. Z., S. M. Li, and F. L. Dou, 2012: Study of obtaining high resolution near-surface atmosphere temperature by using the land surface temperature from meteorological satellite data. *Acta Meteor.*, **70**, 1107–1118, doi: 10.11676/qxxb 2012.093. (in Chinese)

Kusaka, H., F. Chen, M. Tewari, et al., 2012: Numerical simulation of urban heat island effect by the WRF model with 4-km grid increment: An inter-comparison study between the urban canopy model and slab model. *J. Meteor. Soc.*, **90B**, 33–45, doi: 10.2151/jmsj.2012-B03.

Li, J., and A. D. Heap, 2008: A review of spatial interpolation methods for environmental scientists. *Record-Geoscience*, **23**, 137.

Mostovoy, G. V., R. L. King, K. R. Reddy, et al., 2006: Statistical estimation of daily maximum and minimum air temperatures from MODIS LST data over the state of Mississippi. *GISci. Remote*, **43**, 78–110, doi: 10.2747/1548-1603.43.1.78.

Pan, X. D., and X. Li, 2011: Validation of WRF model on simulating forcing data for Heihe River basin. *Sciences in Cold and Arid*, **3**, 344–357, doi: 10.3724/SP.J.1226.2011.00344.

Prihodko, L., and S. N. Goward, 1997: Estimation of air temperature from remotely sensed surface observations. *Remote Sens.*, **60**, 335–346, doi: 10.1016/S0034-4257(96)00216-7.

Qi, S. H., C. F. Luo, C. Y. Wang, et al., 2006: Pre-study on reverse air temperature from remote sensing: Relationship between vegetation index, land surface temperature and air temperature. *Remote Sens. Tech.*, **21**, 130–136, doi: 10.11873/j.issn.1004-0323.2006.2.130. (in Chinese)

Shen, S. H., and G. G. Leptoukh, 2011: Estimation of surface air temperature over central and eastern Eurasia from MODIS land surface temperature. *Environ. Res.*, **6**, 045206, doi: 10.1088/1748-9326/6/4/045206.

Strahler, A., D. Muchoney, J. Borak, et al., 1999: MODIS Land Cover Product Algorithm Theoretical Basis Document (ATBD), Version 5.0. Center for Remote Sensing, Department of Geography, Boston University, Boston, MA, USA. Available online at https://modis.gsfc.nasa.gov/data/atbd/atbd_mod12.pdf, accessed on March 10, 2017, 72 pp.

Wan, Z. M., 1999: MODIS Land-Surface Temperature Algorithm Theoretical Basis Document (LST ATBD). Institute for Computational Earth System Science, Santa Barbara, CA, USA. 75 pp.

Wan, Z. M., 2006: MODIS Land Surface Temperature Products Users' Guide. Institute for Computational Earth System Science, University of California, Santa Barbara, CA, USA Available online at http://www.icess.ucsb.edu/modis/LstUsrGuide/MODIS_LST_products_Users_guide_C5.pdf, accessed on March 10, 2017, 30 pp.

Wan, Z. M., and Z.-L. Li, 2008: Radiance-based validation of the V5 MODIS land-surface temperature product. *Int. J. Remote*, **29**, 5373–5395, doi: 10.1080/01431160802036565.

Wan, Z. M., Y. L. Zhang, Q. C. Zhang, et al., 2004: Quality assessment and validation of the MODIS global land surface temperature. *Int. J. Remote*, **25**, 264–274, doi: 10.1080/0143116031000116417.

Xu, W. H., Q. X. Li, X. L. Wang, et al., 2013: Homogenization of Chinese daily surface air temperatures and analysis of trends in the extreme temperature indices. *J. Geophys.*, **118**, 9708–9720, doi: 10.1002/jgrd.50791.

Xu, W. Y., R. Sun, Z. F. Jin, et al., 2015: Estimation of near surface air temperature based on MODIS data. *Meteor. Environ.*, **38**, 1–6, doi: 10.16765/j.cnki.1673-7148.2015.01.001. (in Chinese)

Zhang, W., Y. Huang, Y. Q. Yu, et al, 2011: Empirical models for estimating daily maximum, minimum, and mean air temperatures with MODIS land surface temperatures. *Int. J. Remote*, **32**, 9415–9440, doi: 10.1080/01431161.2011.560622.

Tech & Copy Editor: Zhirong CHEN
Language Editor: Colin SMITH